

The background of the entire page is a detailed, grayscale image of a microelectronic circuit board. It shows a complex network of fine lines representing traces, larger rectangular pads, and various components like capacitors and integrated circuits. The layout is dense and symmetrical, typical of high-frequency or high-performance electronic designs.

International Journal of

Microelectronics and Computer Science

2010, Volume 1, Number 3

ISSN 2080-8755

Technical University of Łódź, Poland

TABLE OF CONTENTS

A Rapid Analysis of Very Short Channel MOSFET Performances by Using a Dynamic Simple Model <i>A. Rabhi, R. El'Hadj Bekka, A. Benhamadouche, F. Rahmoune, and J.-J. Charlot</i>	225
A Solution to Low Power Switched Capacitor Integrator Design with Reduced Effective Input Capacitance <i>S. Korkmaz, and G. Dundar</i>	229
A sub-μW Conductance Converter for Bioimplantable Devices <i>N. Miranda, and R. Morais</i>	236
Analysis and Design of a MOSFET-only Wideband Balun LNA <i>I. Bastos, L.B. Oliveira, J. Goes, and M. Silva</i>	241
Analysis and Design of CMOS Coupled Multivibrators <i>J. Casaleiro, H.F. Lopes, L.B. Oliveira, and I. Filanovsky</i>	249
Automated Parameter Extraction of Geometry Dependent RF Planar Inductor Model <i>V.P. Durev, E.D. Gadjeva, and M.H. Hristov</i>	257
Automatic Installation of Software-based Fault Tolerance Algorithms in Programs Generated by GCC Compiler <i>A. Piotrowski</i>	263
Digitally Programmable Delay-Locked-Loop with Variable Charge Pump Current <i>B. Lopes, N. Paulino, J. Goes, and A. Steiger-Garção</i>	269
Distributed and Collaborative Product Engineering for MEMS <i>T. Schmidt, K. Hahn, M. Mielke, R. Brück, D. Ortloff, and J. Popp</i>	277
Electro-thermal Co-simulation of ICs with Runtime Back-annotation Capability <i>A. Timár, G. Bognár, A. Poppe, and M. Rencz</i>	287
Hydrogen Bonding Network Emulating Frequency Driven Source of Triangular Pulses <i>R. Rusev, G. Angelov, E. Gieva, M. Hristov, and T. Takov</i>	293
Measurement and Performance Evaluation of a Silicon On Insulator Pixel Matrix <i>D. Ntavelis, L. Harik, J.-M. Sallese, M. Kayal, and A. Hatzopoulos</i>	299
Multichannel Readout System for Registration of Electronic System Temperature Response with High Temporal Resolution <i>M. Janicki, Z. Kulesza, P. Pietrzak, and A. Napieralski</i>	305
Reduced Stress and Fluctuation for the Integrated α-Si TFT Gate Driver on the LCD <i>N.X. Huang, M.S. Shiao, H.-C. Wu, R.C. Sun, and D.-G. Liu</i>	311
Signal Flow Graph Block Approach to the Design of the Universal Mixed-mode Multi-loop Filter and Study of Non-ideal Properties <i>R. Sotner, J. Slezak, T. Dostal, and J. Frydrych</i>	316

Hydrogen Bonding Network Emulating Frequency Driven Source of Triangular Pulses

Rostislav Rusev, George Angelov, Elitsa Gieva, Marin Hristov, and Tihomir Takov

Abstract—A three output microelectronic circuit functionally equivalent to a hydrogen bonding network is modeled. Proton transfer characteristics of each hydrogen bond of the network are emulated by block-elements in the microelectronic circuit with their respective I - V characteristics. These characteristics are coded in Matlab where the dynamic and static analyses are carried out. The results imply that in static mode the functionally analogous circuit operates as a current source or an amplifier. In dynamic mode the circuit behaves as a voltage driven triangular pulse signal source. The simulations show that the generated pulses at the three circuit outputs have different frequency, amplitude, and width.

Index Terms—hydrogen bonding network, proton transfer, microelectronic circuit.

I. INTRODUCTION

THE application of molecular interactions such as hydrogen bonding for design of molecular self-assemble systems in micro- and nanoelectronics, including liquid crystals [1], molecular solids [2], polymeric assemblies [3] has attracted the attention of scientists long time ago. For example, linear porphyrine layers are self-organized through hydrogen bonding coordinated the self-organization of the lipid bi-layer membranes. The electron acceptor is placed on one side of the membrane and the electron donor is placed on the other side. Photo-current arises when the sample is irradiated by white light. The photo-current can be observed only between ordered structures and it cannot be observed between separate molecules. In this way, a photonic electron conductor from simple molecule components can be constructed. On the other hand, the development of such new systems is increasing because the hydrogen bonding in

anisotropic molecular self-assembled structures can form bridges between synthetic materials and/or bio-functional systems. In the biofunctional nature systems, e.g. proteins, the hydrogen bonding is crucial for molecule recognition, molecule stabilization, dynamic reversibility [4], etc. Proton transfer proteins such as Bacteriorhodopsin (bR), which transfers proton current via its own hydrogen bonding network (HBN), might be used for interesting applications in microelectronics. Its proton current versus voltage characteristic is similar to the output characteristic of a microelectronic circuit (differential amplifier) [5].

Similarly to Bacteriorhodopsin we are investigating the possibility for information transfer via branched HBN of β -lactamase protein.

II. MODEL AND EQUATION

The object of the present investigation is a microelectronic circuit similar to β -lactamase branched HBN [6]. The proton transfer parameters of each hydrogen bond are also investigated in [6]. These parameters are the basis of the presented microelectronic simulations in this paper. Here the K -El.pot characteristics of the network (K – proton transfer parameter and El.pot – electrostatic potential) are interpreted as I - V characteristics where the proton transfer parameter is regarded as the electrical current.

The probability for proton transfer from the donor to acceptor is proportional to the value of the K parameter. The proton current between donor and acceptor of each hydrogen bond depends on the K parameter as well. Some authors [7] consider the K parameter to be equivalent to the proton current.

We calculate the proton transfer parameter (K) using the following equations:

$$K = \frac{k_B T}{2\pi} \exp\left(-\frac{E_b - h\omega/2}{k_B T}\right) \quad (1)$$

where: K – proton transfer parameter, k_B – Boltzmann constant, E_b – energy barrier, h – Planck constant, ω – frequency, T – temperature [K].

The energy barrier is calculated by:

$$E_b = (s_A(R(DA) - t_A)^2 + v_A) + s_B E_{12} + (s_C \exp(-t_C(R(DA) - 2)) + v_C)(E_{12})^2 \quad (2)$$

This work was supported by Contract No. D002 – 126/15.12.2008.

R. P. Rusev, PhD is with the Technical University of Sofia, Faculty of Electronics Engineering and Technology (FETT), Dept. of Microelectronics, ECAD Laboratory, phone +359 2 965 3115, fax +359 2 965 2330, rusev@ecad.tu-sofia.bg.

G. V. Angelov, PhD is with the Technical University of Sofia, FETT, Dept. of Microelectronics, ECAD Laboratory, phone +359 2 965 3115, fax +359 2 965 2330, gva@ecad.tu-sofia.bg.

E. E. Gieva, PhD Student is with the Technical University of Sofia, FETT, Dept. of Microelectronics, ECAD Laboratory, phone +359 2 965 3115, fax +359 2 965 2330, gieva@ecad.tu-sofia.bg.

T. B. Takov, PhD, prof. DSc is with the Technical University of Sofia, FETT, Dept. of Microelectronics, ECAD Laboratory, phone +359 2 965 3059, fax +359 2 965 2330, takov@ecad.tu-sofia.bg.

M. H. Hristov, PhD, prof. is with the Technical University of Sofia, FETT, Dept. of Microelectronics, ECAD Laboratory, phone +359 2 965 2220, fax +359 2 965 2220, mhrstov@ecad.tu-sofia.bg.

The branched hydrogen bonding network is represented in Fig. 1 and its functionally analogous electric circuit is shown in Fig. 4.

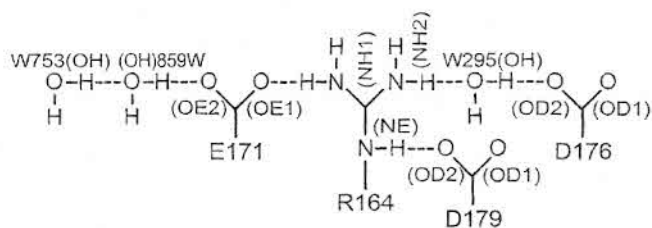


Fig. 1. Magnetization as a function of applied field. Note that "Fig." is abbreviated. There is a period after the figure number, followed by two spaces. It is good practice to explain the significance of the figure in the caption.

The K - V characteristic of each bond is given in Fig. 2 and Fig. 3. It can be observed that the K - V characteristics are non-linear. This allows for the hydrogen bonds to process the signals similarly to the semiconductor devices. On this basis we can construct three- and four-terminal microelectronic block elements that emulate the operation of the hydrogen bonds.

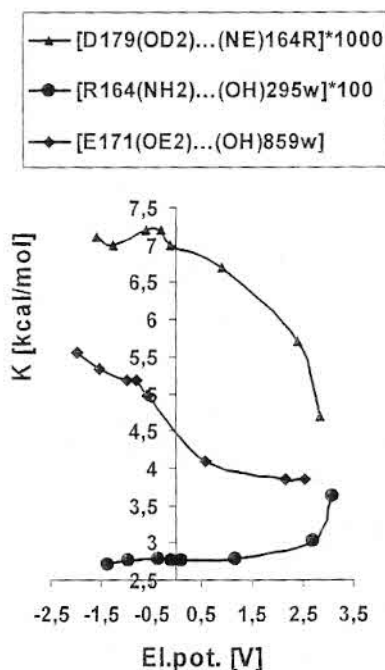


Fig. 2. K - V characteristics of hydrogen bonds: OD2 is oxygen atom of Aspartic acid residue D179, NH2 and NE are nitrogen of Arginine residue R164, OE2 is oxygen atom of Glutamic acid residue E171, and OH is oxygen atom of water molecules w295, w859.

The block elements are based on heavy atoms that are part of the hydrogen bonding network. Each heavy atom simultaneously appears as donor and acceptor in the hydrogen bonding network. In this reason the input of each block element corresponds to the acceptor part of the heavy atom and its output corresponds to the donor part of the heavy atom.

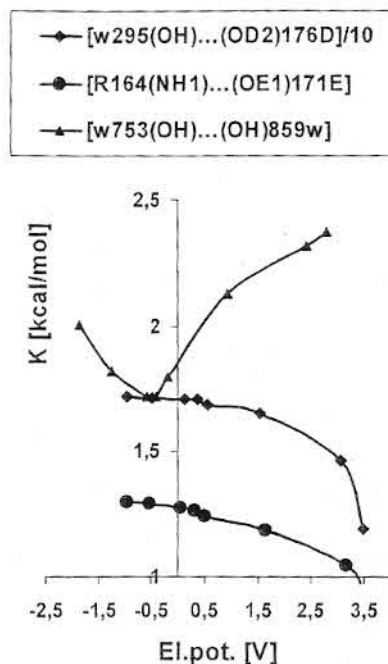


Fig. 3. K - V characteristics of hydrogen bonds: OD2 is oxygen atom of Aspartic acid residue D176, NH1 is nitrogen of Arginine residue R164, OE1 is oxygen atom of Glutamic acid residue E171, and OH is oxygen atom of water molecules w295, w753, w859.

The equivalent circuit composed of these microelectronic block-elements is given in Fig. 4 where each block-element corresponds to a heavy atom in the hydrogen bonding network. The arginine residue R164 is depicted as the four terminal block-element T1. Since it is strong proton donor in the network of hydrogen bonds, in the analogous electric circuit it is represented as voltage-driven current source (with three outputs). Output currents and voltages of T1 are different and they are driven by the input voltage. The second block-element T2 is analogous to aspartic acid residue D179, which is strong proton acceptor. In the electric circuit the block-element T2 is the first output.

Block-elements T4 and T5 are analogous to the input molecule w295 and aspartic acid residue D176 of Fig. 1. They are shown as three-terminal block-elements. Input and output voltages of each of the T4 and T5 block-element are equal and their input but output currents are different. On the other hand T5 is the second circuit output.

The block-element T7 of the circuit is analogous to the strong proton acceptor of HBN E171. It forms two hydrogen bonds with its oxygen OE1 and OE2 atoms: at one of its sides is R164 NH1...(OE1)171E and at the other side is w859 OH...(OE2)171E. The potential on OE2 atom as well as proton current between w859OH and (OE2)171E both depend on the potential of OE1 because of cooperative effect. Consequently, the output current I7 and voltage U7 of the analogous block-element T7 depend on the input voltage U71.

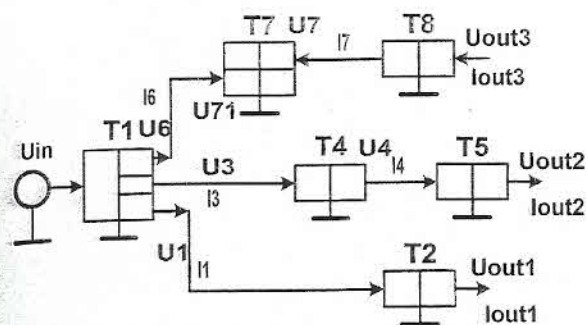


Fig. 4. Magnetization as a function of applied field. Note that "Fig." is abbreviated. There is a period after the figure number, followed by two spaces. It is good practice to explain the significance of the figure in the caption.

The block-element T8 appears to be the last output of the circuit that is analogous to w859 of the HBN. We have to point out that the next water molecule of the HBN, w753, is taken into account but it is not shown in the electrical circuit because the input current to w753 remains the same regardless of how many water molecules are bound after it (under the assumptions of macroscopic model). In this reason we included only block-element T8. Similarly to the other water molecule w295 it is described with three-terminal block-element with identical input and output voltages and different currents.

The relations between currents and voltages of the block-elements in the microelectronic circuit are given by polynomials.

Equation (4) below describes the first output of T1:

$$U1 \in [-1.3:3.2] \text{ step } 0.1 \quad (3)$$

$$I1 = -5.10^{-5} (U1)^3 - 8.10^{-5} (U1)^2 - 2.10^{-5} (U1) + 0.0071 \quad (4)$$

Next are the equations of T2

$$U2 = 0.9994 (U1) - 0.3421 \quad (5)$$

$$I2 = I1 \quad (6)$$

The equation of the second output of T1:

$$U3 = 1.0066 (U1) - 0.0967 \quad (7)$$

$$I3 = 0.0005 (U3)^3 - 0.0006 (U3)^2 - 0.0006 (U3) + 0.028 \quad (8)$$

Equations for T4

$$U4 = 0.9802 (U3) + 0.4294 \quad (9)$$

$$I4 = -0.1922 (U4)^3 + 0.2821 (U4)^2 + 0.0044 (U4) + 16.922 \quad (10)$$

Equations for T5 which is the second output of the circuit

$$U5 = 0.9374 (U4) + 1.4074 \quad (11)$$

$$I5 = I4 \quad (12)$$

Equations of the third output of T1

$$U6 = 1.0193 (U1) + 0.3216 \quad (13)$$

$$I6 = -0.0072 (U6)^3 + 0.0069 (U6)^2 - 0.03 (U6) + 1.2646 \quad (14)$$

Equations of block-element T7

$$U71 = 1.0387 (U6) - 0.5498 \quad (15)$$

$$U7 = 0.9705 (U71) - 0.5167 \quad (16)$$

$$I7 = 0.0591 (U7)^3 + 0.0162 (U7)^2 - 0.6792 (U7) + 4.5597 \quad (17)$$

Equations of T8 that is the third output of the electrical circuit

$$U8 = -0.0437 (U7)^2 + 1.0318 (U7) + 0.4173 \quad (18)$$

$$I8 = 0.0041 (U8)^4 - 0.0456 (U8)^3 + 0.0772 (U8)^2 + 0.234 (U8) + 1.8401 \quad (19)$$

```
plot(U7,U8,'linewidth',2);
grid on
set(gca,'fontweight','b','fontsize',14)
title('T8');
xlabel('U7 [V]');
ylabel('U8 [V]');
% legend('simulation','data');
set(legend('\bf simulation',
'\bf data',1),'fontsize',12);
pause;

% I8=f(U8) in p1
I8 = 0.0041*U8.^4 - 0.0456*U8.^3 + 0.0772*U8.^2
+ 0.234*U8 + 1.8401;

load('fig7_1btl_w753.dat');
U8exp = fig7_1btl_w753(:,1);
I8exp = fig7_1btl_w753(:,2);

plot(U8,I8,U8exp,I8exp,'ro','linewidth',2);
grid on
set(gca,'fontweight','b','fontsize',14)
title('T8');
xlabel('Uout3 [V]');
ylabel('Iout3 [pA]');
% legend('simulation','data');

set(legend('\bf simulation',
'\bf data',1),'fontsize',12);
pause;
```

Fig. 5. An excerpt of the Matlab code for simulation of the equivalent circuit behavior.

These equations are coded in Matlab where the static and dynamic analyses of the microelectronic circuit are performed [8]. Sample Matlab code is given in Fig. 5.

III. STATIC ANALYSIS

The static analysis is performed by feeding input voltage U_{in} between -1.3 and $+3.2$ [V]. Subsequently, a comparison between I-V characteristics of each block-element and the proton transfer characteristics of the respective hydrogen bond from paper [6] is carried out. Sample results of the juxtaposition are depicted on Fig. 6 and 10; for the other block-elements the results are similar and they are not shown on the figures. As it can be seen, the polynomials well describe the hydrogen bond functions. The maximal standard deviation from all simulations versus data set is ± 4.33 %. The model is in good agreement with the experimental data for hydrogen bonds because standard deviation of the measurements is in the range of 4% to 12%.

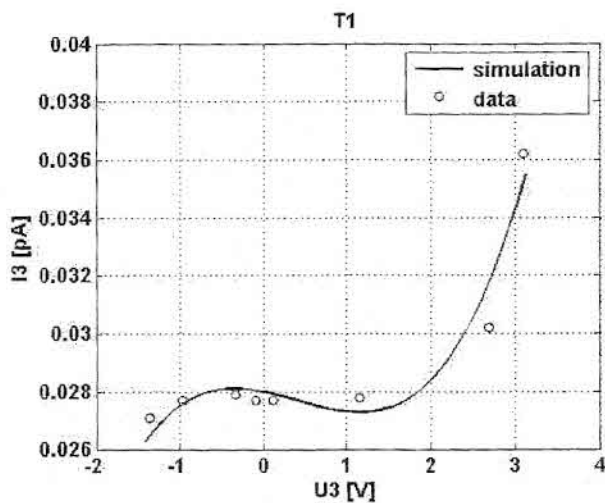


Fig. 6. Simulation versus data set of T1 block-element.

Still, the simulations show that all output voltages are proportional to the input voltage (Fig. 7). U_{out1} and U_{out3} are almost equal and U_{out2} is shifted up. When U_{in} is varied between -1.3 and $+3.2$ [V] then U_{out1} and U_{out3} are changing in interval $-1.5 \div +3.2$ [V], and U_{out2} is increasing from 0.5 to 4.5 [V].

In contrast to the voltages, the currents are always positives. The currents of the different outputs are changing in different intervals from 10^{-3} to 10^1 [pA]. The I-V characteristics of output 1 and output 2 have similar forms (Figs. 8 and 9) but they are shifted to one another. For output 1: when U_{out1} is in the interval between -1.5 and 0 [V] I_{out1} is constant.

Consequently, this circuit can be used as current source. When U_{out1} is varying between 0 and $+3$ [V] the current is decreasing, i.e. this output is similar to the output of an amplifier. By analogy such conclusions can be made also for output 2: the circuit operates as current source at $U_{out2} = +0.5$ to $+2.5$ [V] because the I_{out2} current is stable. When U_{out2} is between $+2.5$ to $+4.5$ [V], the output of the circuit is again similar to an amplifier output.

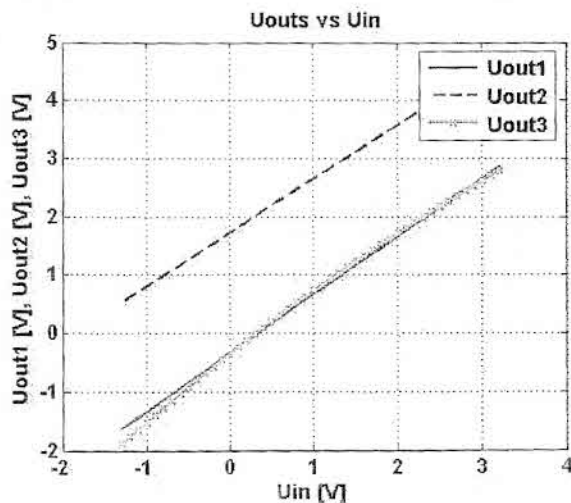
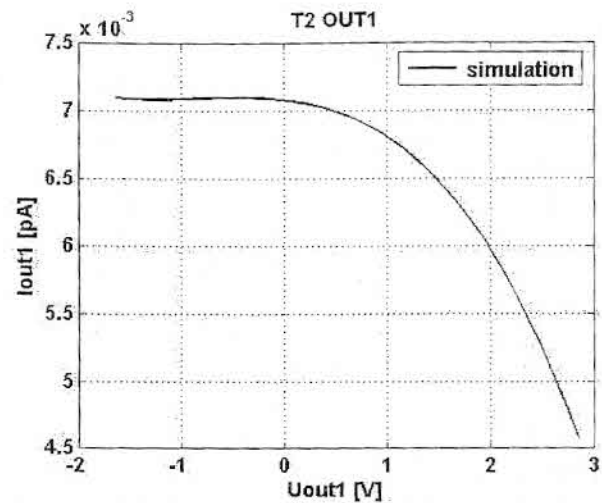
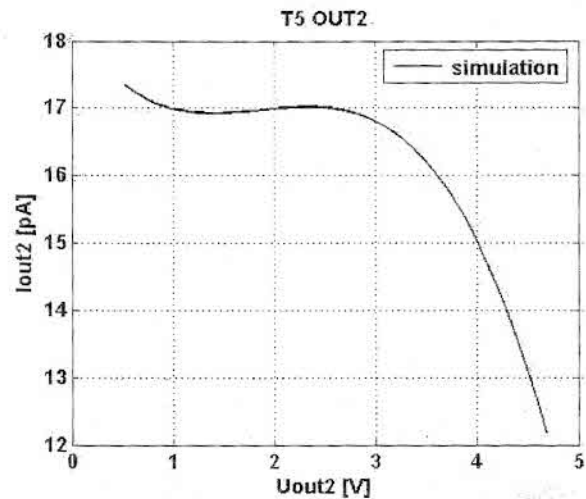
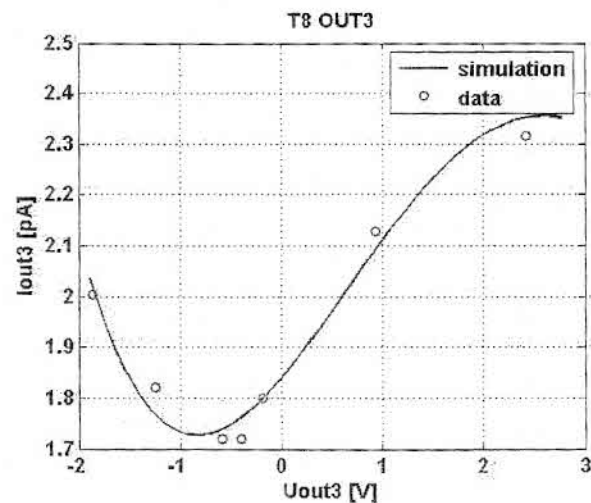


Fig. 7. Outputs voltages versus input voltage.

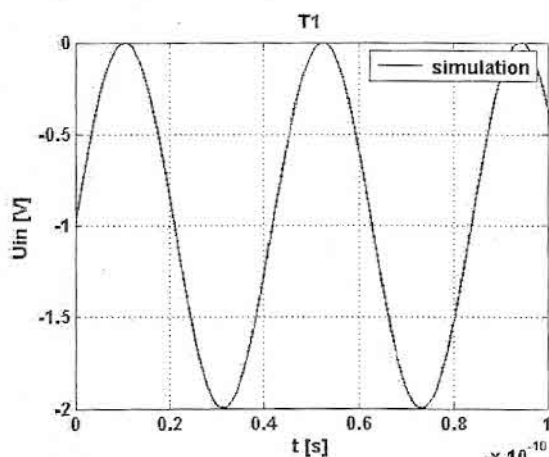
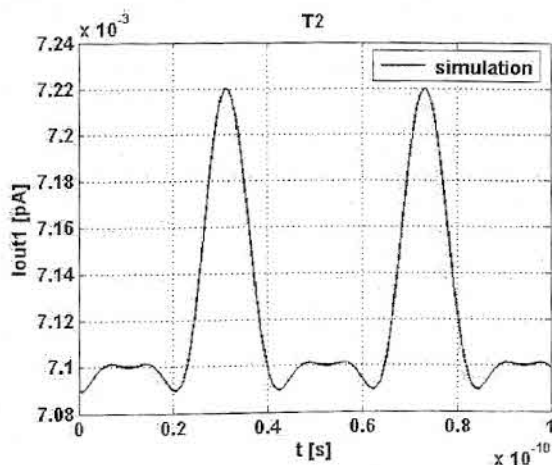
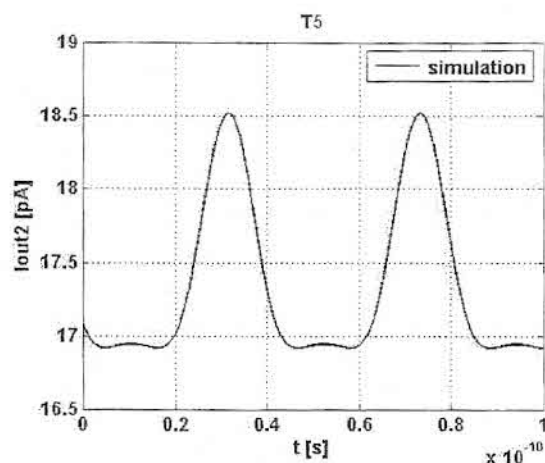
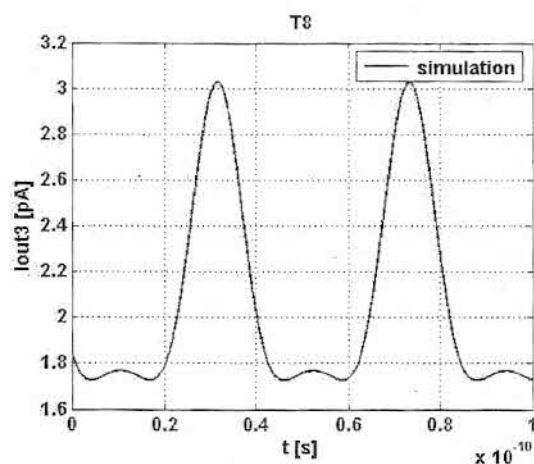
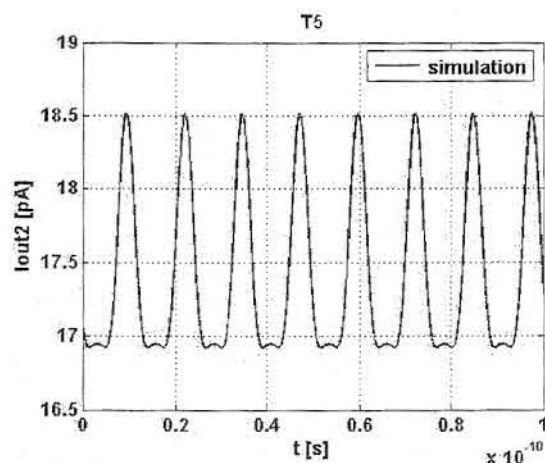
Fig. 8. First output characteristics: I_{out1} vs. U_{out1} .Fig. 9. Second output characteristics: I_{out2} vs. U_{out2} .Fig. 10. Third output characteristics: I_{out3} vs. U_{out3} .

IV. DYNAMIC ANALYSIS

The dynamic analysis is done by transient simulations in the range $0 \div 10^{-10}$ [s] because in nature objects proton transfers durations are in these time intervals. Subsequently the analogous microelectronic circuit should operate at much higher frequencies — ca. 10 [GHz]. The circuit is tested with sine input voltages with different amplitudes and frequencies. At $U_{in} = 1.5 \times \sin(t \times 5 \times 10^{11})$ the outputs have characteristics (not shown in the paper) and the circuit operates as signal modulator producing signals with different amplitude and form.

At $U_{in} = -1 + \sin(t \times 1.5 \times 10^{11})$ stable circuit operation is observed (Fig. 11): at the three outputs triangular pulses are generated (Figs. 12, 13, 14).

Figures show that the pulses are with equal frequency, phase, and positive amplitude. The three pulses are with different amplitudes and the width of the pulses at the first output is less than the width of the pulses at outputs 2 and 3. On the other hand we can control the period of the output pulses by changing the period of the input voltage. For instance, on Fig. 15 is given characteristic of I_{out2} versus time that is obtained at $U_{in} = -1 + \sin(t \times 5 \times 10^{11})$, analogous to the characteristics obtained at the other outputs. By comparing Figs. 13 and 15 it can be seen that the triangular pulses of Fig. 15 are with larger frequency. Similar result is observed for the other outputs and thence they are not shown.

Fig. 11. U_{in} versus time.Fig. 12. I_{out} vs. time at $U_{in} = -1 + \sin(t \times 1.5 \times 10^{11})$.Fig. 13. I_{out2} vs. time at $U_{in} = -1 + \sin(t \times 1.5 \times 10^{11})$.Fig. 14. I_{out3} vs. time at $U_{in} = -1 + \sin(t \times 1.5 \times 10^{11})$.Fig. 15. I_{out2} vs. time at $U_{in} = -1 + \sin(t \times 5 \times 10^{11})$.

Finally, the microelectronic circuit that is analogous network of hydrogen bonds can operate as frequency source of triangular pulses. The three outputs generate pulses with different amplitude and width.

V. CONCLUSION

The hydrogen bonding network model proved that such biofunctional system has real microelectronics applications. The analogous microelectronic circuit may operate in static mode as a current source or an amplifier. In dynamic mode the microelectronic circuit may function as a voltage driven triangular pulse signal generator. At the three circuit outputs might be generated pulses with different frequency, amplitude, and width. Thus, the biocircuit appears to be extremely flexible and is applicable to multiple circuit purposes.

REFERENCES

- [1] T. Kato, "Supramolecular liquid-crystalline materials: molecular self-assembly and self-organization through intermolecular hydrogen bonding", *Supramolecular Science*, vol. 3, issues 3 pp. 53-59, 1996.
 - [2] D. Lawrence, T. Jiang, M. Levett, "Self-Assembling Supramolecular Complexes", *Chem. Rev.*, Vol. 95, pp.2229-2260, 1995.
 - [3] S. Stupp, V. LeBonheur, K. Walker, L. S. Li, K. E. Huggins, M. Keser, and A. Amstutz, "Supramolecular Materials: Self-Organized Nanostructures," *Science*, vol. 276, pp. 384-389, 1997.
 - [4] G A Jeffrey, "An Introduction to Hydrogen Bonding Book Description," Oxford University Press, USA, pp 320, 1997.
 - [5] D. Braun, N.A. Dencher, A. Fahr, M. Lindau, and M.P. Heyn, "Nonlinear Voltage Dependence of the Light-Driven Proton Pump Current of Bacteriorhodopsin," *Biophysical Journal*, vol. 53, pp. 617 - 621, 1988.
 - [6] R. Rusev, G. Angelov, T. Takov, B. Atanasov, M. Hristov, "Comparison of Branching Hydrogen Bonding Networks with Microelectronic Devices", *Annual J. of Electronics*, Vol.3, No. 2, pp. 152-154, 2009
 - [7] Brunger A., Z. Schulten and K. Schulten. A Network Thermodynamic Investigation of Stationary and non-Stationary Proton Transport through Proteins. *Z. Phys. Chem.*, 1983, vol. 136, pp. 1-63.
 - [8] Matlab website <http://www.mathworks.com>.
- Rostislav P. Rusev** is born on 27.11.1976 in Svishtov. He obtained a Master of Engineering Physics degree from Sofia University St. Kliment Ohridski, Sofia, Bulgaria in 2002 and defended his PhD thesis at the Technical University of Sofia, Bulgaria in 2010.
- George V. Angelov** (M'2004) is born on 19.02.1976 in Sofia. He obtained a Master of Physics degree from Sofia University St. Kliment Ohridski, Sofia, Bulgaria in 1999 and defended his PhD thesis at the Technical University of Sofia, Bulgaria in 2008. He worked for the Technology Centre-Institute of Microelectronics between 1999-2001 as modeling researcher, and Hybrid Integrated Circuits between 2001-2003 as process engineer and quality manager. Since 2007 he is assistant professor at the Technical University of Sofia, Dept. of Microelectronics.
- Elitsa E. Gieva** is born on 03.06.1982 in Ruse. She obtained a Master of Electronics Engineering degree from Tehnical University of Sofia, Sofia, Bulgaria in 2009 and she is PhD student at the Technical University of Sofia, Bulgaria in 2010.
- Tihomir B. Takov** is born on 28.02.1945. He obtained a Master of Engineering from Saint Petersburg Electrotechnical University, Russia in 1968 and his PhD and Doctor of Science degrees from Technical University of Sofia, Bulgaria in 1975 and 1989 respectively. He joined the Institute of Semiconductor Devices in Botevgrad, Bulgaria, where he was engaged in research and development of semiconductor devices and integrated circuits; he became director of the Institute of Microelectronics and Optoelectronics, Botevgrad, Bulgaria in 1974. Prof. Dr. T. Takov is currently professor in Dept. of Microelectronics at the Technical University of Sofia and of the National Highest Accreditation Commission.
- Marin H. Hristov** is born on 15.11.1949. He obtained a Master of Engineering and PhD degrees from the Technical University of Sofia, Bulgaria in 1972 and 1979 respectively. He became assistant professor in the Dept. of Electronics at Technical University of Sofia, Bulgaria in 1976, associate professor and full professor at the Dept. of Microelectronics in 1986 and 2004 respectively. He was Dean of the Faculty of Electronic Engineering and Technology between 1989-1995 and Vice Rector of the Technical University of Sofia between 1999-2005. Prof. Dr. Marin H. Hristov is currently professor in Dept. of Microelectronics at the Technical University of Sofia and Dean of the Faculty of Electronic Engineering and Technology.